

# On the Microhardness of Silicon Nitride and Sialon Ceramics

A. K. Mukhopadhyay, S. K. Datta & D. Chakraborty

Central Glass and Ceramic Research Institute, P.O. Jadavpur University, Calcutta 700 032, India

(Received 30 December 1989; revised version received 16 May 1990; accepted 28 May 1990)

## Abstract

*Influences of relative density, grain size, Young's modulus, flexural strength and fracture toughness on microhardness characteristics of hot-pressed silicon nitride, sintered silicon nitride, reaction-sintered sialon and liquid-phase sintered sialon have been discussed. Three new semi-empirical equations have been proposed to correlate microhardness to relative density. Indentation size effects on microhardness measurement have also been discussed.*

*Die Abhängigkeit der Mikrohärtigkeit von heißgepreßtem, gesintertem und reaktionsgesintertem Siliziumnitrid sowie flüssigphasen-gesintertem Sialon von der rel. Dichte, Korngröße, Elastizitätsmodul, Biegefestigkeit und Bruchzähigkeit wurde untersucht. Es wurden drei neue, halbempirische Gleichungen aufgestellt, die die Mikrohärtigkeit mit der rel. Dichte in Bezug setzen. Auf die Abhängigkeit der Mikrohärtigkeit von der Größe des Härteeindrucks wird ebenso eingegangen.*

*On discute ici de l'influence de la densité relative, de la taille des grains, du module de Young, de la résistance en flexion et de la ténacité sur la microdureté des matériaux suivants: nitrure de silicium fritté naturellement ou pressé à chaud et sialon élaboré par frittage réactif ou frittage en phase liquide. On propose trois nouvelles équations semi-empiriques reliant la microdureté à la densité relative et l'on discute également de l'effet de la taille de l'indent sur les mesures effectuées.*

## 1 Introduction

The hardness characterisation of dense silicon nitride ( $\text{Si}_3\text{N}_4$ ) and sialon ceramics is extremely

important for their thorough exploitation as low-cost cutting tool materials replacing costly super-alloy-based products currently in use. Hot-pressed silicon nitride (HPSN), sintered silicon nitride (SSN), reaction-sintered sialon (RS sialon) and the liquid-phase sintered sialon (LPS sialon) offer the most promising candidature for such applications.

Regarding the microhardness of these materials, the following information is available. Single crystal  $\alpha$ -silicon nitride is harder than single crystal  $\beta$ -silicon nitride, the prismatic planes are harder than the basal plane in the  $\alpha$ -silicon nitride and the presence of residual  $\alpha$ -phase improves the microhardness of the polycrystalline dense silicon nitride.<sup>1–4</sup> Reduction in the amount of sintering additive, flexural strength and average grain size have been related to improvement in microhardness of HPSN.<sup>5–7</sup> In the case of SSN the porosity,  $\alpha$ -phase content and elastic modulus are reported to affect the microhardness,<sup>8,9</sup> but it is not significantly influenced by post-sintering heat treatment<sup>9</sup> and the choice of sintering aids.<sup>10</sup> Microhardness improvement has been induced with reduction in substitution level of RS sialon<sup>11</sup> and LPS sialon.<sup>12</sup> Crystallisation of the grain boundary phase has also led to microhardness improvement in the latter type of sialon.<sup>13</sup>

It is often very difficult to make any quantitative comparisons between published microhardness results for a given silicon nitride or sialon ceramic because of differences in density and load range used by different workers.<sup>1–13</sup> The problem of density difference can be partially overcome if a quantitative correlation between microhardness and relative density exists. There clearly exists a lack of information on grain size and mechanical properties dependence of microhardness in the case of SSN and sialon ceramics.<sup>8–13</sup> The purpose of the present work was: (a) to correlate relative density and

microhardness; (b) to study grain size dependence of microhardness; (c) to elucidate the association of flexural strength, fracture toughness and Young's modulus with microhardness; (d) to examine if microhardness bears any relation to the width of the indentation crack; (e) to generate a Knoop microhardness database and compare the same with Vickers microhardness; and (f) to identify the threshold load beyond which indentation size effects have negligible influence on microhardness.

## 2 Experimental

### 2.1 Materials

The HPSN samples with 2.5 wt%  $Y_2O_3$  were commercially obtained. The sintering liquid system for SSN samples M2, M3, M3A, M3B, RM3 was  $Y_2O_3$ -AlN-SiO<sub>2</sub>, for samples M4, M5, M5A, M5B it was MgO-AlN-SiO<sub>2</sub> and for sample M6 it was MgO-SiO<sub>2</sub>. The sintering liquid system for LPS sialon samples M8, M8A, M8B, M9 was  $Y_2O_3$ -AlN-SiO<sub>2</sub> and for sample M10 it was MgO-SiO<sub>2</sub>. The basic raw material for synthesis of SSN and sialon materials was  $Si_3N_4$  powder prepared in-house by nitridation of Si.<sup>14</sup> The  $Si_3N_4$  powder had BET surface area  $8.8 \text{ m}^2 \text{ gm}^{-1}$ , about 86 wt%  $\alpha$ -phase and chemical analysis (wt%) of: N, 38.63; O, 2.2; K, 0.31; Ca, 0.053; Mg, 0.01; Na, 0.084 and Fe, 0.143 as obtained by standard conventional methods.<sup>15</sup> In the general formula  $Si_{6-z}Al_zO_zN_{8-z}$  for sialon, Z represents the number of oxygen atoms substituting nitrogen in the silicon nitride lattice. The starting compositions of the present RS sialon and LPS sialon ceramics were adjusted to Z values of 1.0 and 0.5 respectively.<sup>16</sup> The RS sialon was prepared from a stoichiometric powder mixture of  $Si_3N_4$ , AlN and  $Al_2O_3$ . The LPS sialon samples were synthesised using the RS sialon powder and the proper amounts of sintering aids.

The green billets of SSN and sialon samples were sintered inside BN-coated graphite crucibles at 1700–1800°C for 30–90 min in pure nitrogen atmosphere in a graphite resistance furnace (Astro, USA). Post-sintering heat treatment of the SSN samples M3 and M5 in the temperature range of 1330–1430°C for 30–180 min in pure nitrogen atmosphere led to synthesis of the crystallised SSN samples RM3 and RM5 respectively.<sup>15,17</sup>

The density ( $d$ ) was measured by the water immersion technique utilising Archimedes' principle. The relative density ( $d'$ ) was calculated as  $d_{\text{measured}}/d_{\text{theoretical}}$ . A theoretical density of  $3.2 \times 10^3 \text{ kg m}^{-3}$  on average was assumed<sup>7,13</sup> for all the

Table 1. Grain size of HPSN, SSN and Sialon Ceramics

	Sample	Grain size ( $\mu\text{m}$ )
HPSN	M1	—
	M1A	1.66
	M1B	—
SSN	M2	3.97
	M3	2.05
	M3A	—
	M3B	2.66
	RM3	—
	M4	2.33
	M5	—
	M5A	1.68
	M5B	—
	RM5	1.55
M6	1.80	
RS Sialon	M7	2.78
LPS Sialon	M8	—
	M8A	—
	M8B	2.33
	M9	2.13
	M10	2.00

— = Not determined.

materials. Grain size data given in Table 1 were estimated by the linear intercept method from numerous SEM photographs of polished as well as etched sections.<sup>16,17</sup> The etching was done at 350°C for 40–80 min in molten NaOH salt. Crystalline phase identification by conventional XRD techniques showed  $\beta$ - $Si_3N_4$  and  $\beta'$ -sialon as major phases in various SSN and sialon ceramics respectively.

### 2.2 Methods

From the hot-pressed and sintered billets samples of size  $15 \times 10 \times 5 \text{ mm}^3$  were cut. The samples were mounted in resin and subjected to grinding by SiC powders. Finally, they were polished with  $1 \mu\text{m}$  diamond paste.

The polished samples were subjected to Vickers and Knoop diamond pyramid indentation under loads of 1N, 2N, 5N, 10N and 20N in a Leitz miniload hardness tester. From the start of the controlled release of the indenter onto the specimen surface to the development of a well-defined indentation impression on the same surface took about 30 s. All the tests were carried under ambient laboratory conditions. The Vickers microhardness value ( $H_V$ ) was calculated using the relation  $H_V = 1854.4 F/d_0^2$ , where  $F$  is the indentation load and  $d_0$  is the indentation diagonal. The Knoop microhardness value ( $H_K$ ) was estimated using the formula  $H_K = 14229 F/d_0^2$ . For each specimen at least 15 measurements were made and 3–5 specimens were

used for each result of  $H_V$  and  $H_K$ . The average of the two indentation diagonals was taken as the value of the indentation diagonal in each individual calculation of  $H_V$ . In the case of  $H_K$  calculation, however, the longest diagonal was taken. The degree of scatter in each data set was estimated by the percentage coefficient of variation given by definition<sup>1</sup> as [(standard deviation/arithmetic mean)]  $\times$  100. The presence of the indentation size effect was examined using the relation

$$F = ad_0^N \quad (1)$$

where  $a$  and  $N$  are experimental parameters of complex significance.<sup>6</sup>

For evaluation of Young's modulus ( $E$ ),<sup>18</sup> flexural strength ( $\sigma$ ) and fracture toughness ( $K_{IC}$ )<sup>14-17</sup> under ambient conditions, rectangular bars ( $45 \times 4.5 \times 3.5 \text{ mm}^3$ ) and a high-temperature bending strength tester (model 422s, Netzsch, FRG) were used. The samples were surface-finished as mentioned in Section 2.1. Young's modulus was evaluated by the static beam bending method,<sup>19</sup> flexural strength by a four-point bending test and fracture toughness by the single edge notched beam (SENB) technique.<sup>7,13</sup> Four to six specimens were used to determine the data of each mechanical property of each sample. Average scatter of data was less than 10%. To evaluate  $K_{IC}$  by the SENB technique the notch length was kept at 0.3-0.6 of the sample width. Further details of experimental methods are given in the authors' previous publications.<sup>14-18</sup>

The indentation crack widths were measured on scanning electron micrographs of polished, indented and subsequently etched surfaces. An indentation load of 10N was used. Etching was done as mentioned in Section 2.1.

### 3 Results and Discussion

Table 2 contains the data on sample number, load, indentation diagonal,  $H_V$  values with the percentage coefficient of variation, relative density ( $d'$ ), Young's modulus ( $E$ ), flexural strength ( $\sigma$ ) and fracture toughness, [ $K_{IC}$ (SENB)] for the HPSN, SSN and sialon ceramics. Data given in Table 2 and Fig. 1 show that  $H_V$  measured at 10N load results in an almost load-independent value of microhardness. Due to this fact microhardness measured at 10N load has been used for comparison purpose of different materials in this work.

Table 2 shows that the HPSN M1 sample (relative density 1) has the highest microhardness value of all the samples examined in the present work. However,

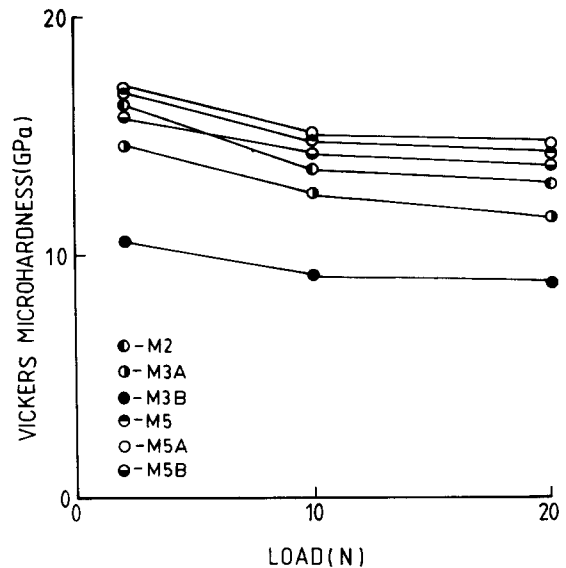


Fig. 1. Variation of Vickers microhardness with load for SSN ceramics.

at a comparable relative density microhardness of HPSN and LPS sialon are similar (compare samples M1A and M8, Table 2). However, even at a comparable relative density the microhardness of SSN is lower than that of HPSN (compare samples M5 and M1B, Table 2). A similar conclusion is reached also for RS sialon (compare samples M7 and M1B, Table 2). Out of all the SSN and sialon products, the SSN M5A and the LPS sialon M8 show the highest microhardness in their respective categories. Crystallised SSN samples RM3 and RM5 show microhardness similar to those of the corresponding parent SSN samples M3 and M5 respectively. This indicates that the post-sintering heat treatment did not significantly influence the microhardness of SSN M3 and M5. Similar results have been reported by other workers.<sup>9</sup> The data of Table 2 further show that SSN M2 has microhardness higher than M3, although both have similar types of sintering additives. Similarly SSN M5 has a microhardness higher than that of SSN M4, although both have similar types of sintering additives.

It will be shown in the following discussion that quite a number of material characteristics, viz. relative density, grain size, Young's modulus, strength, etc., may influence the microhardness. As most of the variables are interdependent on each other, an absolute isolation of their individual influence on microhardness could not be done. On the contrary, they are found to influence the microhardness values in combination. The discussions of present results are made keeping this fact in view.

**Table 2.** Vickers microhardness, relative density and mechanical properties of HPSN, SSN and sialon

Sample	Relative density	Vickers microhardness (GPa) <sup>a</sup>	Load (N)	Indentation diagonal ( $\mu\text{m}$ )	Young's modulus (GPa)	Flexural strength (MPa)	Fracture toughness ( $\text{MPa m}^{1/2}$ ) <sup>b</sup>
M1	1.00	16.2 (2)	10	33.5	310	—	—
M1A	0.99	18.9 (2)	1	9.8	277	—	—
		17.5 (1)	2	14.4			
		16.0 (2)	5	23.8			
		15.6 (2)	10	34.1			
M1B	0.98	18.3 (3)	1	9.9	249	—	—
		17.5 (1)	2	14.7			
		15.4 (1)	5	24.3			
		15.5 (2)	10	34.3			
M2	0.97	15.9 (4)	2	15.1	251	478	6.59
		13.3 (4)	10	36.9			
		12.7 (3)	20	53.4			
M3	0.95	12.7 (4)	10	37.8	207	310	6.20
M3A	0.94	14.3 (6)	2	15.9	207	294	5.76
		12.3 (7)	10	38.4			
		11.3 (5)	20	56.7			
M3B	0.89	10.5 (6)	2	18.6	191	242	4.57
		9.1 (4)	10	44.8			
		8.6 (6)	20	65.2			
RM3	0.95	13.0 (3)	10	37.4	209	—	5.70
M4	0.96	13.9 (5)	10	36.1	350	487	6.08
M5	0.98	16.5 (2)	2	14.8	236	314	3.43
		14.4 (2)	10	35.5			
		13.9 (3)	20	50.2			
M5A	0.97	16.6 (2)	2	14.8	227	—	4.66
		14.7 (2)	10	35.1			
		14.3 (4)	20	50.5			
M5B	0.96	15.5 (4)	2	15.3	—	—	—
		13.9 (5)	10	36.2			
		13.4 (3)	20	52.1			
RM5	0.98	16.2 (2)	2	15.0	223	299	4.71
		14.5 (3)	10	35.1			
		14.0 (2)	20	51.0			
M6	0.95	15.5 (4)	2	15.3	248	311	3.75
		13.7 (3)	10	36.5			
		12.9 (3)	20	52.1			
M7	0.98	15.0 (3)	5	24.6	238	309	3.37
		14.0 (4)	10	36.1			
		14.0 (2)	20	51.0			
M8	0.98	15.7 (3)	10	34.0	227	370	6.80
M8A	0.94	16.8 (2)	2	14.7	269	255	—
		13.8 (5)	10	36.3			
		13.4 (2)	20	52.0			
M8B	0.93	14.5 (1)	2	15.8	243	271	4.84
		12.0 (1)	10	38.9			
		11.7 (2)	20	55.8			
M9	0.93	14.7 (4)	2	15.8	247	—	5.20
		13.1 (2)	10	37.3			
		11.4 (3)	20	56.4			
M10	0.93	14.6 (1)	2	15.8	241	221	4.21
		12.7 (3)	10	37.8			
		11.9 (4)	20	55.2			

<sup>a</sup> Digits in parentheses represent percentage coefficient of variation of Vickers microhardness.

<sup>b</sup>  $K_{IC}$  (SENB) data (taken from Refs 14, 15 and 16).

— = Not determined.

**3.1 Effect of relative density on microhardness**

The data presented in Table 2 show that, in general, the microhardness measured at 10N load increases with increase in relative density. For example, the relative density ( $d'$ ) of the HPSN materials M1, M1A and M1B can be classified as  $d'$  of M1 >  $d'$  of M1A >  $d'$  of M1B and their microhardness ( $H$ ) can be classified as  $H$  of M1 >  $H$  of M1A >  $H$  of M1B. Similar analogy holds good in the cases of SSN and sialon samples (Table 2). To explain the effect of relative density on microhardness a quantitative relationship must exist between the two.

Now, it is known that microhardness ( $H$ ) is related to the indentation diagonal  $d_0$  as<sup>20</sup>

$$H = ad_0^{m-2} \tag{2}$$

Since  $d_0$  is related inversely to the material's characteristic Newtonian resistance  $R_m$  against deformation, then

$$H = a_1[f(R_m)]^M \tag{3}$$

where  $a_1$  is a parameter,  $f(R_m)$  is a suitable function of  $R_m$  and the parameter  $M = 2 - n$ . On the basis of reported experimental evidence<sup>21-23</sup> and present results,  $R_m$  is proposed to be proportional to some function of mass per unit volume of deformation zone, i.e. relative density ( $d'$ ), some function of bond strength per unit area ( $S_b$ ) and some function of fracture surface energy ( $\gamma$ ). Thus

$$R_m \propto f_1(d') \tag{4}$$

$$R_m \propto f_2(S_b) \tag{5}$$

and

$$R_m \propto f_3(\gamma) \tag{6}$$

i.e.

$$R_m \propto f_4(d', S_b, \gamma) \tag{7}$$

Now, putting eqn (4) in eqn (3)

$$H = a_2[f_5(d')]^M \tag{8}$$

where  $a_2$  is a parameter. In particular, if  $M = 1$ , a linear relationship between microhardness and relative density could be obtained. Otherwise, a power law relation would be expected from eqn (8). However, the choice of an exponential function of relative density would lead to an exponential relationship. Based on these considerations the following three semi-empirical equations relating microhardness to relative density are proposed:

$$H = a'_1(d') \tag{9}$$

$$H = a'_2(d')^{n_1} \tag{10}$$

$$H = a'_3 \exp(a'_4 d') \tag{11}$$

**Table 3.** Influence of relative density on microhardness

Proposed equation	Method	Parameters	$\chi^2$	Correlation coefficient
$H = a'_1(d')$	LLS <sup>a</sup>	$a'_1 = 14.4$	2.2	0.95
$H = a'_2(d')^{n_1}$	LLS	$a'_2 = 12.7;$ $n_1 = -0.2$	2.8	0.94
$H = a'_3 \exp(a'_4 d')$	LLS	$a'_3 = 0.19;$ $a'_4 = 4.49$	0.47	0.94

<sup>a</sup> Linear least square.

where  $a'_j$  values ( $j = 1, 2, 3, 4$ ) and  $n_1$  are empirical parameters.

Least-square fitting of the relative density–microhardness data presented in Table 2 to eqns (9), (10) and (11) was done to assess their comparative performance. The results are given in Table 3 along with  $\chi^2$  estimates and correlation coefficients calculated by standard statistical methods.<sup>24</sup> On the basis of the least  $\chi^2$  estimate criteria, it may be concluded from the data of Table 3 that the exponential equation

$$H = [0.19 \exp(4.49d')] \pm 0.55 \text{ (GPa)} \tag{12}$$

describes the present data best. Applicability of eqn (12) is demonstrated in Fig. 2 wherein Vickers microhardness of RBSN<sup>1</sup> and HPSN<sup>6</sup> could be predicted pretty close to actual experimental data using eqn (12). The microhardness and relative density data of Refs 1 and 6 were not used in deriving eqn (12). Therefore, eqn (12) did not carry any influence of those literature data<sup>1,6</sup> but could still predict microhardness pretty close to actual experimental data on the basis of relative density only.

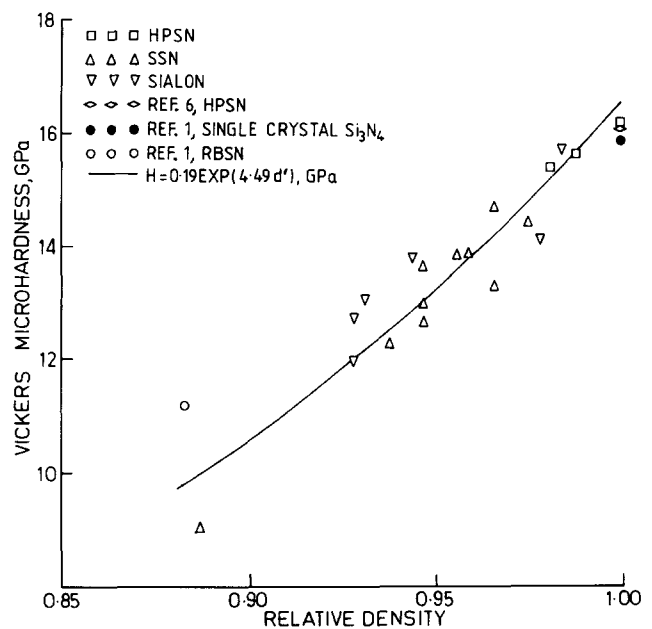


**Fig. 2.** Relationship between relative density and Vickers microhardness of various Si<sub>3</sub>N<sub>4</sub> and sialon ceramics.

Thus, eqn (12) can be used to compare literature data on microhardness of various  $\text{Si}_3\text{N}_4$  ceramics reported by different researchers. The same equation can be further utilised in giving a rough idea of the microhardness of a laboratory-grade  $\text{Si}_3\text{N}_4$  product, on the basis of relative density measurements only. Therefore, eqn (12) can be advantageously exploited from the quality-control viewpoint also.

### 3.2 Influence of grain size on microhardness

It may be noted from Table 2 that at comparable relative density, SSN sample M5A shows microhardness higher than that of SSN sample M2. The situation with SSN samples M6 and M3 and the LPS sialon sample M10 and M8B is similar. Inspection of the data of Tables 1 and 2 reveals that in each pair of above-mentioned ceramics, higher microhardness was associated with lower average grain size. Therefore, it appears that apart from chemical composition and relative density, grain size could also be a factor contributing towards microhardness variation.

To examine whether a general trend of microhardness improvement with reduction in average grain size exists for the present  $\text{Si}_3\text{N}_4$  and sialon ceramics, the average grain size data from Table 2 and Vickers microhardness data measured at 10N load of corresponding ceramics from Table 2 were fitted to the following equations:<sup>20</sup>

$$H = H_0 + K(G)^{-0.5} \quad (13)$$

$$H = H_0 + K \ln(G) \quad (14)$$

where  $H$  is microhardness,  $G$  is average grain size, and  $H_0$  and  $K$  are empirical parameters. Equations (13) and (14) are reported<sup>20</sup> to be valid only for the cases where the indentation zone of influence is large enough to correctly encounter the presence of grain boundaries. If it is smaller than the grain size, it can no longer feel the grain boundaries and consequently the microhardness becomes independent of the grain size.<sup>20</sup> In the present data SSN sample M2 with the largest average grain size ( $3.97 \mu\text{m}$ ) has an indentation diagonal of  $36.9 \mu\text{m}$  at 10N load. The indenter zone of influence is at least three times the indentation diagonal,<sup>25</sup> i.e.  $\sim 110.7 \mu\text{m}$ . So it would accommodate at least  $110.7 \mu\text{m}/3.97 \mu\text{m}$  or about 27 grains of average size and consequently, at least 26 grain boundaries. This information justifies the applicability of eqns (13) and (14) to the present data.

On least-square fitting eqns (13) and (14) yield  $\chi^2$  estimates of 1.89 and 1.95 respectively. On the basis of minimum  $\chi^2$  estimate criteria, then, eqn (13)

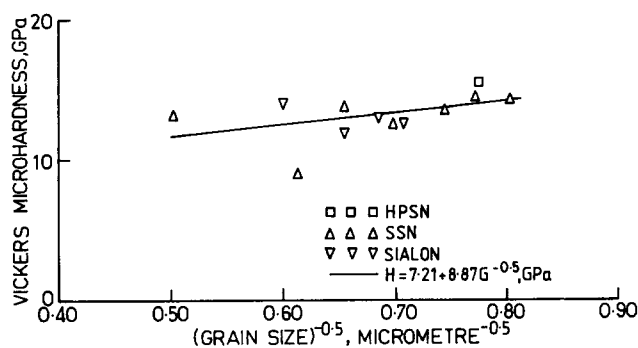


Fig. 3. Grain size versus Vickers microhardness of HPSN, SSN and sialon ceramics.

represents the present data better than eqn (14) does, and the best fitted line shown in Fig. 3 represents the equation

$$H = [7.22 + 8.87(G)^{-0.5}] \pm (0.14)\text{GPa} \quad (15)$$

Figure 3 clearly demonstrates the presence of a general trend of microhardness improvement with reduction in average grain size.

### 3.3 Dependence of microhardness on mechanical properties

Using the data from Table 2, Figs 4, 5 and 6 indicate that for the present ceramics there is a definite correspondence between the Young's modulus, flexural strength and fracture toughness [ $K_{IC}(\text{SENB})$ ] on the one hand and Vickers microhardness on the other. The corresponding indentation load is 10N. Figure 4 shows an increasing trend of microhardness with Young's modulus. The solid line in Fig. 4 represents the best fitted straight line of the form

$$H = [8.44 + 0.02E] \pm (1.40)\text{GPa} \quad (16)$$

having a  $\chi^2$  estimate of 2.75. At nearly equal strength values, the SSN samples M5 and RM5 show similar microhardness (Fig. 5). At nearly equal fracture toughness values, the SSN samples M3 and RM3

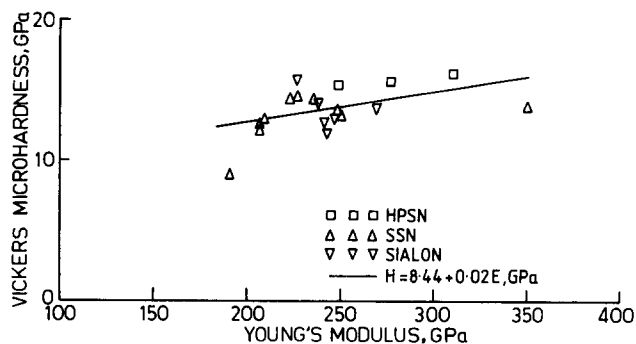


Fig. 4. Relationship between Young's modulus and Vickers Microhardness of the HPSN, SSN and sialon ceramics.

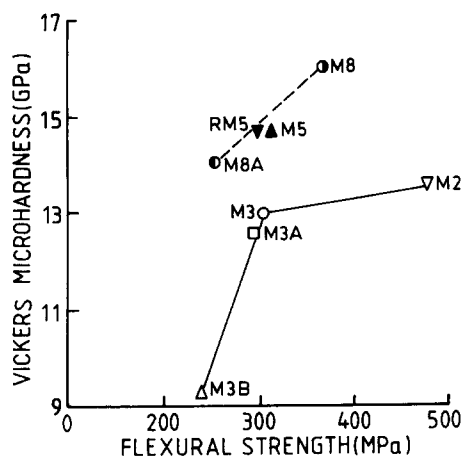


Fig. 5. Relationship between strength and Vickers microhardness of the SSN and sialon ceramics.

show similar microhardness (Fig. 6). The correspondence between strength and fracture toughness on one hand and microhardness on the other is most prominent for the samples M2, M3, M3A, M3B, RM3 of SSN and M8, M8A, M8B, M9, M10 of LPS sialon, but the correspondence is not significantly prominent in the cases of SSN samples M4, M5 and M5A (Figs 5 and 6).

### 3.4 Knoop microhardness of SSN and sialon ceramics

Table 4 presents Knoop microhardness data measured at 10N load of the present SSN and sialon ceramics. Out of the seven SSN samples used for Knoop microhardness measurement the SSN samples M3B and RM5 show the lowest and highest microhardness respectively. Out of the five LPS sialon products tested similarly, the samples M8 and M8B show the highest and lowest Knoop microhardness respectively. Of all the SSN and sialon samples taken together the LPS sialon sample M8 has the highest Knoop microhardness. The data of

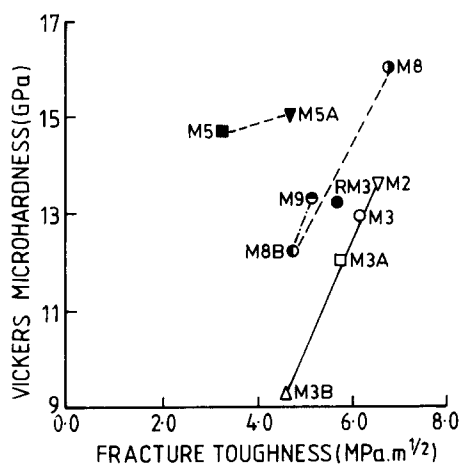


Fig. 6. Dependence of Vickers microhardness on fracture toughness of the SSN and sialon ceramics.

Table 4. Comparison of Vickers and Knoop microhardness for SSN and sialon

Sample	$H_V$ (GPa) <sup>a</sup>	$H_K$ (GPa) <sup>a</sup>	$H_V/H_K$
M2	13.3 (4)	12.2 (2)	1.09
M3A	12.3 (2)	11.0 (4)	1.12
M3B	9.1 (4)	8.5 (6)	1.07
RM3	13.0 (3)	12.3 (1)	1.06
M5	14.4 (2)	12.8 (2)	1.13
M5B	13.9 (3)	12.5 (3)	1.11
RM5	14.5 (3)	12.8 (4)	1.13
M8	15.7 (4)	13.8 (1)	1.14
M8A	13.8 (5)	12.3 (2)	1.12
M8B	12.0 (2)	11.3 (1)	1.06
M9	13.1 (2)	11.3 (2)	1.15
M10	12.7 (5)	11.6 (3)	1.09

<sup>a</sup> Digits in parentheses represent percentage coefficient of variation.

Table 4 show further that at an indentation load of 10N, the Knoop microhardness of the present ceramics are in general lower than the corresponding Vickers microhardness values. In fact the ratio of Vickers to Knoop microhardness varies from 1.06 to 1.15, with a mean of 1.105 and standard deviation of  $\pm 0.03$ . The importance of this calibration factor (i.e. 1.105) can easily be realised from the fact that using this factor allows prediction of Knoop microhardness data from the Vickers microhardness measurement and vice versa. Most of the literature data are expressed either as Vickers microhardness<sup>1-3,6-7</sup> or as Knoop microhardness<sup>8</sup> values and such conversion factors are rarely available in literature.

### 3.5 Indentation crack widths of SSN and sialon

Experimental measurements of indentation crack width (not to be confused with crack length) in SSN<sup>14</sup> samples yield values of 0.22, 0.20, 1.80, 1.86, 0.33 and 0.16  $\mu\text{m}$  for samples M2, M3, M4, M5A, RM5 and M6 respectively. Similarly, LPS sialon samples M8, M9 and M10 have indentation crack widths<sup>14</sup> of 0.45, 0.45 and 0.18  $\mu\text{m}$  respectively. Figures 7 and 8 show typical examples of indentation cracks in SSN sample M5A and crystallised SSN sample RM5 respectively. The crystallised SSN sample RM5 has an indentation crack width (Fig. 8) about six times smaller than that of the as-sintered parent SSN sample M5 (Fig. 7). Similarly the width of indentation cracks in SSN sample M2 and M3 is about nine times lower than those of the SSN sample M4 and M5. Out of all the SSN samples, the material M6 with sintering aids from the MgO-SiO<sub>2</sub> system (Table 1) has the lowest indentation crack width. The same sintering liquid is related to the lowest

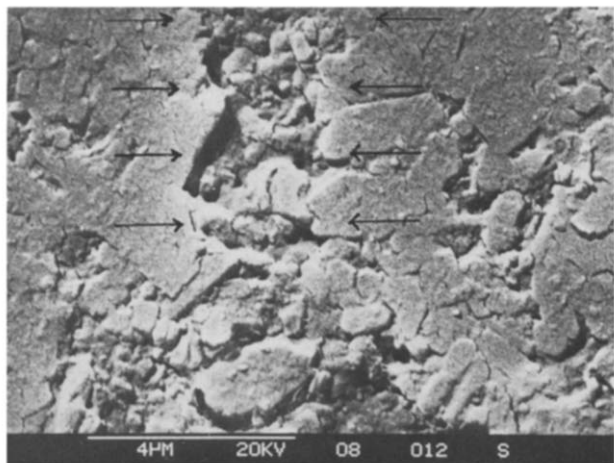


Fig. 7. Indentation crack in the SSN sample M5A. Width of crack marked with arrow.

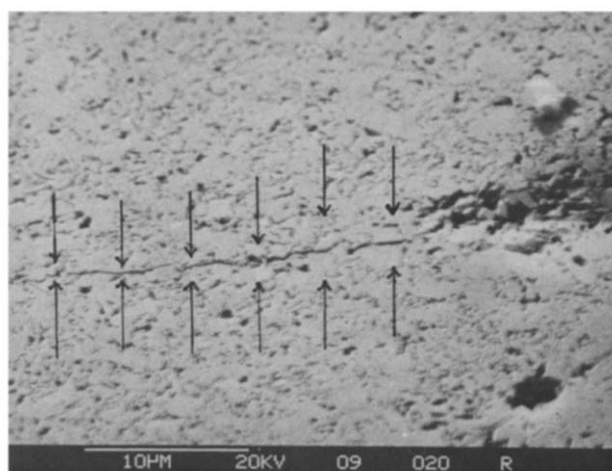


Fig. 8. Indentation crack in the crystallised SSN sample RM5. Width of crack marked with arrow.

indentation crack width of  $0.18 \mu\text{m}$  in the LPS sialon sample M10 also. At comparable relative density, however, irrespective of starting composition, it appears that ceramics with lower width of indentation cracks possess higher values of Vickers microhardness. It may be pointed out that no such observation on correlation of crack width with microhardness has ever been reported by any worker prior to this work.

### 3.6 Indentation size effect

The increase in microhardness with decreasing load, i.e. indentation size effect,<sup>20,25</sup> appears to be present in this case (Table 2). Plots of load ( $F$ ) versus indentation diagonal ( $d_0$ ) ( $\ln-\ln$ ) were drawn for all the studied materials and typical examples are shown in Fig. 9(a) and (b) for the HPSN sample M1A and SSN sample M5 respectively. The dotted lines in Fig. 9 were obtained for fixed values of  $N=2$  in eqn (1). Such an  $N$  value is reported<sup>6</sup> to be characteristic of hard, brittle materials. At  $F \geq 10\text{N}$ ,

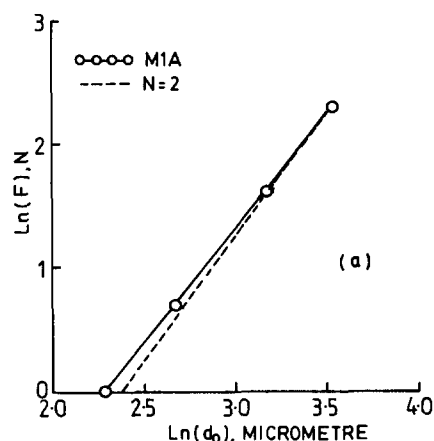
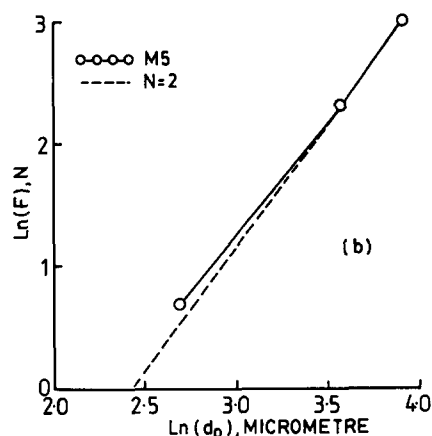


Fig. 9. Load versus Indentation diagonals of (a) HPSN sample M1A and (b) SSN sample M5.

the experimentally obtained line either shows a negligibly small difference to the line for  $N=2$  (Fig. 9(a)) or practically coincides asymptotically with it (Fig. 9(b)). At  $F < 10\text{N}$  the experimentally obtained lines show a finite difference with the line for  $N=2$ . Similar curves for other materials (not shown in Fig. 9) exhibited a similar behaviour. From this evidence it appears most likely that  $10\text{N}$  is the threshold load level at and above which the indentation size effect would have negligible influence on measured microhardness. For the present materials, the load-dependence character of indentation diagonals (Fig. 9) is very much within the framework of general load versus diagonal curves as indicated by Bückle's model.<sup>25</sup> According to Bückle,<sup>25</sup> the presence of 'coherent regions' in the material is responsible for the observed increase in microhardness with decreasing load and 'coherent regions' may have the significance of grain volume.

## 4 Summary and Conclusions

- (i) Out of HPSN, SSN, RS sialon and LPS sialon HPSN shows the highest value of Vickers microhardness.

- (ii) Vickers microhardness measured at 10N load for the presently studied materials show an increasing trend with relative density, (grain size)<sup>-0.5</sup> and Young's modulus. Three new semi-empirical equations, viz.  $H = a'_1(d')$ ,  $H = a'_2(d')^{n_1}$  and  $H = a'_3 \exp(a'_4 d')$  have been proposed to correlate microhardness ( $H$ ) and relative density ( $d'$ ). In particular the equation  $H = 0.19 \exp(4.49 d')$  GPa describes the present data best.
- (iii) Improvements in flexural strength and fracture toughness, [ $K_{IC}(\text{SENB})$ ] on the one hand and Vickers microhardness on the other, have direct correspondence in the cases of present SSN and sialon ceramics.
- (iv) Post-sintering heat treatment causes no significant change in Vickers microhardness of SSN but a nearly six-fold reduction in indentation crack width occurs in crystallised SSN.
- (v) To avoid an unwanted contribution of indentation size effect on measured Vickers microhardness, indentation loads of 10N or greater should be used in the cases of materials similar to those used in the present work.

### Acknowledgement

Thanks are due to the members of the High Temperature Materials Laboratory, Central Glass and Ceramic Research Institute, for supplying some of the samples. Thanks are also due to Dr (Mrs) S. Sen for SEM work and to Mr S. N. Chatterjee for photographic work. The authors thank the Director, CG&CRI for his keen interest in this paper.

### References

1. Chakraborty, D. & Mukerji, J., Characterization of silicon nitride single crystals and polycrystalline reaction sintered silicon nitride by microhardness measurements. *J. Mater. Sci.*, **15** (1980) 3051.
2. Greskovich, C. & Yeh, H. C., Hardness of dense  $\beta$ -Si<sub>3</sub>N<sub>4</sub>. *J. Mater. Sci. Lett.*, **2** (1983) 657.
3. Greskovich, C. & Gazza, G. E., Hardness of dense  $\alpha$ - and  $\beta$ -Si<sub>3</sub>N<sub>4</sub> ceramics. *J. Mater. Sci. Lett.*, **4** (1985) 195.
4. Nihara, K. & Hirai, T., Hardness anisotropy of  $\alpha$ -Si<sub>3</sub>N<sub>4</sub> single crystal. *J. Mater. Sci.*, **13** (1978) 2276.
5. Tsuge, A. & Nishida, K., High-strength hot-pressed Si<sub>3</sub>N<sub>4</sub> with concurrent Y<sub>2</sub>O<sub>3</sub> and Al<sub>2</sub>O<sub>3</sub> additions. *Amer. Ceram. Soc. Bull.*, **57** (1978) 424.
6. Babini, G. N., Bellosi, A. & Galassi, C., Characterization of hot-pressed silicon nitride based materials by microhardness measurements. *J. Mater. Sci.*, **22** (1987) 1687.
7. Coe, R. F., Lumby, R. J. & Powson, M. F., Some properties and applications of hot-pressed silicon nitride. In *Special Ceramics*, Vol. 5, ed. P. Popper. British Ceramic Research Association, Stoke-on-Trent, UK, 1972, pp. 361–76.
8. Prochazka, S. & Greskovich, C. D., Sintered silicon nitride for high-performance applications. Final Report under Contract No. DAAG 46-77-C-0030., General Electric Company, Schenectady, New York, 1978.
9. Chakraborty, D. & Mukerji, J., Study on fracture toughness and Vickers microhardness of Si<sub>3</sub>N<sub>4</sub>, SiC, sialon and Al<sub>2</sub>O<sub>3</sub>. In *Powder Metallurgy and Related High-Temperature Materials*, ed. P. Ramkrishna. Oxford and IBM Publishing Company, India, 1985, pp. 288–95.
10. Pasto, A. E., Neil, J. T. & Quackenbush, C. L., Microstructural effects influencing strength of sintered silicon nitride. In *Ultra-Structure Processing of Ceramics, Glasses and Composites*, ed. L. L. Hench & D. R. Ulrich. John Wiley & Sons, NY, 1984, pp. 476–87.
11. Briggs, J., Pressureless sintering of sialon ceramics. *Mater. Res. Bull.*, **12** (1977) 1047.
12. Lumby, R. J., The variation of hardness in Lucas Syalon ceramics. *J. Mater. Sci. Lett.*, **2** (1983) 345.
13. Lumby, R. J., Preparation and properties of commercial sialon materials. *Ceram. Eng. Sci. Proc.*, **3** (1982) 50.
14. Mukhopadhyay, A. K., Study on parameters influencing fracture toughness of silicon nitride and its composites. PhD thesis, Jadavpur University, Calcutta, India, 1987.
15. Mukhopadhyay, A. K., Chakraborty, D. & Mukerji, J., High-temperature fracture toughness and fractographic study of dense Si<sub>3</sub>N<sub>4</sub>. In *High Tech Ceramics*, ed. P. Vincenzini. Elsevier, Amsterdam, 1987, pp. 1325–33.
16. Mukhopadhyay, A. K. & Chakraborty, D., High-temperature fracture toughness and fractographic study of reaction sintered and liquid-phase sintered sialon. *Mater. Sci. Eng.*, **A104** (1988) 215.
17. Chakraborty, D. & Mukhopadhyay, A. K., Creep of sintered silicon nitride. *Ceram. Int.*, **15** (1989) 237.
18. Chakraborty, D. & Mukhopadhyay, A. K., High-temperature Young's modulus of reaction-bonded silicon nitride, liquid-phase sintered silicon nitride and sialon. *Ceram. Int.*, **14** (1988) 127.
19. Jayatilaka, A. De S. & Leake, J. A., Influence of progressive oxidation on Young's modulus and fracture toughness of reaction-bonded silicon nitride. *Proc. Brit. Ceram. Soc.*, **25** (1975) 311.
20. Braunovic, M., Effect of grain boundaries and free surfaces. In *The Science of Hardness Testing and Its Research Application, Symposium of the American Society for Metals*, ed. J. H. Westbrook & H. Conrad. American Society for Metals, Metal Park, OH, 1977, pp. 329–76.
21. Gilman, J. J., Hardness—a strength microprobe, In *The Science of Hardness Testing and Its Research Application, Symposium of the American Society for Metals*, ed. J. H. Westbrook & H. Conrad. American Society for Metals, Metals Park, OH, 1977, pp. 51–74.
22. Plendl, J. N. & Gielisse, P. J., Hardness of nonmetallic solids on an atomic basis. *Phys. Rev.*, **125** (1962) 828.
23. Rice, R. W., Correlation of hardness with mechanical effects in ceramics. In *The Science of Hardness Testing and Its Research Application, Symposium of the American Society for Metals*, ed. J. H. Westbrook & H. Conrad. American Society for Metals, Metals Park, OH, 1977, pp. 117–34.
24. Kenny, J. F. & E. S. Keeping, *Mathematics of Statistics, Part I*; Van Nostrand, Princeton, NJ, 1954, pp. 197–8.
25. Bückle, H., Use of the hardness test to determine other material properties. In *The Science of Hardness Testing and Its Research Application, Symposium of the American Society for Metals*, ed. J. H. Westbrook & H. Conrad. American Society for Metals, Metal Park, OH, 1977, pp. 453–94.